Available online at www.sciencedirect.com
ScienceDirect
Mechatronics 18 (2008) 218–230
MECHATRONICS

Design and evaluation of an active electromechanical wheel suspension system

Mats Jonasson [a,b,*], Fredrik Roos [c]

[a] Department of Chassis and Vehicle Dynamics, Volvo Car Corporation, SE-405 31 Göteborg, Sweden
[b] KTH Vehicle Dynamics, SE-100 44 Stockholm, Sweden
[c] KTH Mechatronics, SE-100 44 Stockholm, Sweden

Received 18 June 2007; accepted 26 November 2007

Abstract

This paper presents an electromechanical wheel suspension, where the upper arm of the suspension has been provided with an electric levelling and a damper actuator, both are allowed to work in a fully active mode. A control structure for the proposed suspension is described. The complex design task involving the control of the electric damper and its machine parameters is tackled by genetic optimisation. During this process, these parameters are optimised to keep the power dissipation of the electric damper as low as possible, while maintaining acceptable comfort and road-holding capabilities. The results of the evaluations carried out demonstrate that the proposed suspension can easily adopt its control parameters to obtain a better compromise of performance than that offered by passive suspensions. If the vehicle is to maintain acceptable performance during severe driving conditions, the damper has to be unrealistically large. However, if the electric damper is combined with a hydraulic damper, the size of the electric damper is significantly reduced. In addition, the design of the electric damper with the suggested control structure, including how it regenerates energy, is discussed.

Keywords: Automotive; Active suspensions; Electric vehicles; Electric dampers

1. Introduction

Conventional vehicles are typically equipped with hydraulic dampers and helical springs to isolate the car body from road irregularities and to ensure sufficient contact between tyre and road. This type of passive wheel suspension is tuned to act within an acceptable compromise between comfort and road holding, due to fixed suspension parameters [1]. The need for rapid adjustments of the on-board suspension characteristics for various driving dynamics and driver preferences has resulted in an increasing interest in active solutions. Normally, comfort at a high level is desired. However, if for some reason, the tyre adhesion available deteriorates, the suspension needs to rapidly adjust its parameters to the new situation to address road holding at the expense of comfort. In addition, active systems are able to supply mechanical power to each corner of the vehicle in order to dynamically adjust heave, roll and pitch motions.

Fully active suspensions, in contrast to semi-active solutions, are allowed to work in *all* quadrants in a force-velocity graph (see Fig. 1). This is solved by one, or more, force-producing actuators between the wheel and the car body. Apart from dissipating energy during damping cycles, the actuators must also be able to inject energy into the wheel suspension if needed. If the active suspension is implemented by the electric actuators, it may even be possible to recover energy when operating in the regenerative mode of the actuator. The amount of energy regenerated depends on the actual road condition and actuator control structure applied. During the regenerative mode, energy

* Corresponding author. Address: Department of Chassis and Vehicle Dynamics, Volvo Car Corporation, SE-405 31 Göteborg, Sweden. Tel.: +46 31 592918.
E-mail address: mjonass2@volvocars.com (M. Jonasson).

0957-4158/$ - see front matter © 2007 Elsevier Ltd. All rights reserved.
doi:10.1016/j.mechatronics.2007.11.003

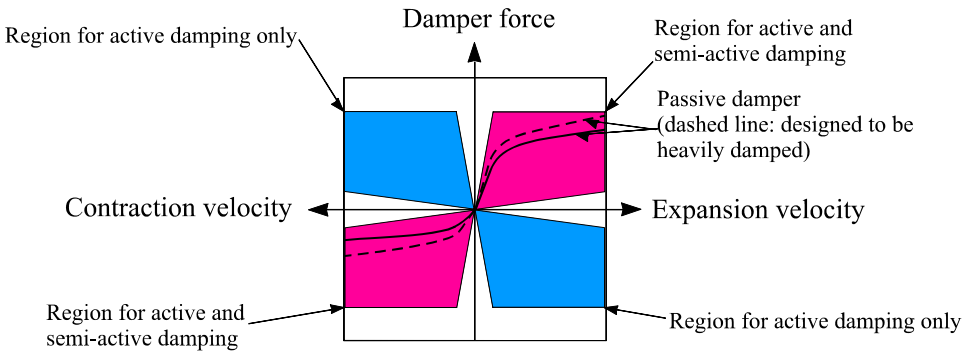

Fig. 1. Force–velocity regions for active, semi-active and passive damping. Here, the velocity is the relative speed between the car body and the wheel.

can be stored in the energy buffers of the vehicle. Nevertheless, the regenerated energy is gained at the expense of higher longitudinal motion resistance, which can affect the driveline energy consumption of the vehicle [2].

A large part of the work presented in this paper deals with the parameter optimisation of the active suspension system. Extensive research has previously been published within the field of active suspension optimisation. In [3], both actuator and control parameters are optimised simultaneously. However, actuator power limitations and actuator dynamics are not incorporated in the optimisation process used, which might lead to unrealistic design solutions. In [4], the actuator power consumption is weighted to be included in the objective function. However, the physical limitation of the actuator is not considered here. Research findings from [5] demonstrate the optimisation of the *Skyhook* parameters, though the spring and damper parameters are fixed. Consequently, most of the previous research findings suffer from not optimising the constrained actuator, and as a result, the true system optimum cannot be reached.

The key challenge associated with active suspension and electromechanical actuators is size, weight and energy consumption required to achieve acceptable performance. For this reason, the physical properties of the actuator are to be included in the optimisation problem. The purpose of this paper is to evaluate the performance of the new suspension proposed, but in addition, to optimise and to analyse the size, weight and energy consumption of the suspension actuator required to achieve that performance.

1.1. Contributions and outline of paper

In this paper, the feasibility of introducing an electromechanical wheel suspension in vehicles is examined by analysing the electric damper proposed, its physical size, performance and electrical power needed. A method to determine the suspension and control parameters during the predevelopment process is thoroughly outlined. The electromechanical wheel suspension is then evaluated and compared with a passive wheel suspension by investigating their responses to tyre force excitations.

Firstly, a suitable control structure is proposed for the electric wheel suspension. By re-expressing the rotational dynamics of the electric damper into linear motions, the well established quarter car model can be employed. Secondly, performance indices of the wheel suspension are formulated. Thirdly, the dimensioning of the electric damper, springs and control parameters are determined through a three-step optimisation process. It is shown that the electric damper needs to be large, if it is to withstand severe driving conditions. Finally, by elaborating the damper performance indices used in the optimisation process, this paper demonstrates how the electric damper responds to tyre force excitations for three different sets of design parameters.

This paper is outlined as follows: Section 2 describes the active suspension design studied. The dynamic modelling of the suspensions under consideration is presented in Sections 3 and 4 describes the control structure used. Section 5 formulates the rotational dynamics of the upper arm of the active suspension and its actuators. The dimensioning and optimisation process is described in Section 6. Finally, the evaluation and conclusions are presented in Sections 7 and 8, respectively.

2. Active suspension design

The active suspension studied is part of the Autonomous Corner Module (ACM), which was invented at Volvo Car Corporation (VCC) in 1998 [6,7]. In 2005, the invention was further developed and the damper became entirely electromechanical [8]. The upper arm of the wheel suspension, which is normally passive and bounded by suspension kinematics, has been provided with an active function. As seen in Fig. 2a–c, this function has been implemented by attaching two actuators to the end of the upper arm. Since the existing arm can be used for actuation, additional suspension linkages are not needed to incorporate the active function and, in turn, fewer parts are required. In addition, the constitution of rotational actuators is better matched to electrical machines, since these have the potential to be smaller than their linear counterparts.

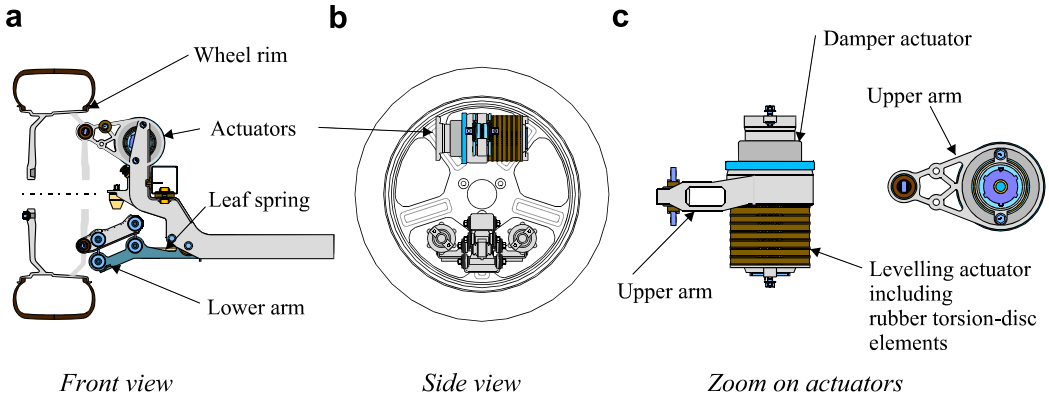

Fig. 2. A design proposal of the active suspension design, which originates from an ACM (illustrations reproduced with kind permission from Sigvard Zetterström at KTH, Sweden) [6,7].

In this case, two electrical machines provide the active function; one actuator is designed to work as a damper, while another alters the vertical position of the car body (see Fig. 2c). The machine housings are attached to the upper arm and their centre shafts are both connected to the car body. The damper actuator is composed of an electrical machine combined with a gearhead only. The levelling actuator consists of a number of identical rubber torsion-disc elements, which can be pretensioned by an electrical machine combined with a gearhead. The damper and the levelling actuator can be controlled separately to support a desired torque to the upper arm. However, to relieve the vertical arm from static vertical forces, a leaf spring is attached to the lower arm of the wheel suspension.

The characteristics of conventional wheel suspension mainly depends on the invariable component parameters (such as spring rate), which are tuned to perfection through the development of the vehicle. Normally, these front and rear parameters differ: rear springs are more rigid to be able to withstand a variety of loadings from the luggage compartment and also to ensure a low level of transient pitch motion when negotiating bumps on the road. These demands on different parameters between the front and the rear make it difficult to keep the total number of wheel suspension components low. Nevertheless, the hardware specification of the electromechanical wheel suspension proposed can be similar for all four corners. This is made possible by the software-controlled levelling actuator: levelling adjustments are done by pretensioning its torsion spring and instead, the transient response is transformed into a control issue (the spring rate may be considered to be manipulated).

3. Modelling the suspension configurations

This section specifically focuses on the vertical dynamics of each corner of the vehicle only. Within the confines of this paper, dynamics which involve the car body states and the corner interactions are intentionally ignored and the wheel suspension can be represented by the well established quarter car model. Furthermore, the performance of the active suspension studied is compared with a passive state-of-the-art solution and thus, the modelling of both configurations is considered.

The quarter car model is a two-degree-of-freedom system, which includes the sprung mass, m_b, the unsprung mass, m_w, and their corresponding vertical positions, z_b, and, z_w, respectively. However, the approach used is restricted to modelling the tyre as a linear spring with a specific stiffness, k_w, while the tyre damping is intentionally ignored. The road irregularity, z_{road}, is regarded as a disturbance, which excites the tyre vertically.

The non-linear quarter car model can now be expressed as

$$\begin{aligned} m_b\ddot{z}_b &= F_{susp} - m_b g \\ m_w\ddot{z}_w &= -F_{susp} - m_w g + k_w(z_{road} - z_w) \\ z_{deflection,min} &< z_{road} - z_w < z_{deflection,max} \end{aligned} \tag{1}$$

where $z_{deflection,min}$ and $z_{deflection,max}$ are limitations of tyre belt deflections and g is the gravitational constant. The suspension force, F_{susp}, is dependent on the actual suspension configuration.

3.1. Passive suspension

When examining the conventional passive suspension, as seen in Fig. 3a, a linear spring with a stiffness, $k'_{b,}$ is employed where the' symbol indicates that the parameter is valid for passive suspensions only, as well as a non-linear damper with a damping force, F_d. Accordingly, the suspension force for the passive configuration becomes

$$\begin{aligned} F_{susp} &= F_d + k'_b(z_w - z_b) \\ F_d &= F_d(\dot{z}_{rel}), \quad \dot{z}_{rel} = \dot{z}_w - \dot{z}_b \\ z_{rel,min} &< z_{rel} < z_{rel,max} \end{aligned} \tag{2}$$

The force induced from the passive damper is strongly dependent on the sign and the magnitude of the relative velocity, $\dot{z}_{rel}$ between the sprung and the unsprung masses. This non-linear relation, which is illustrated in Fig. 4, has

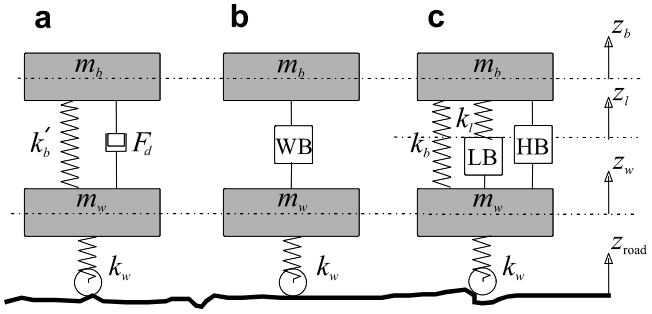

Fig. 3. Wheel suspension represented by a quarter car model for: (a) a conventional passive system, (b) an active abstraction and (c) the active suspension studied.

been measured on a hydraulic damper designed for a mid-size premium car. Moreover, this graph illustrates the results of the piecewise linearisation technique adopted for the purpose of modelling.

3.2. Active suspensions

Bearing in mind the arrangement of the rotational actuators proposed and described in Section 2, these do not move along a vertical axis 'up and down' as described for the quarter car model. However, before examining this issue further (Section 5), the actuators are first presumed to move linearly (Sections 3 and 4), as in the quarter car description. One abstraction of an active wheel suspension, as shown in Fig. 3b, can be seen as a wheel suspension equipped with an actuator (denoted as WB = wide bandwidth) between the sprung and unsprung masses. This actuator takes on the role as the passive spring and damper. From Eq. (1), it is evident that when the suspension force $F_{\text{susp}} = -m_b g$ that the velocity of the sprung mass is cancelled out. However, this approach means that the control of the unsprung mass velocity fails. In addition, the limitation of the maximum and minimum suspension travel allowed makes this approach impossible. When using this approach in practice, it is also difficult to design an electric actuator without a significant need for power, and in turn, this leads to a large amount of dissipated energy. This problem can partially be solved by introducing a spring, similar to the one used in conventional suspensions. Thus, the spring relieves the static load of the vehicle from the actuator.

The linear counterpart of the suspension configuration proposed in this paper, which is shown in Fig. 3c, benefits from the use of one electric levelling actuator (denoted as LB = low bandwidth in Fig. 3c) and one electric damper actuator (denoted as HB = high bandwidth in Fig. 2c). The former benefits from levelling the vehicle and actively altering the level of the car body corners during the roll and pitch motions induced. Since these activities are relatively slow, approximately 1–5 Hz, the bandwidth requirement of the levelling actuator may still be operated at a low level. There is a built-in self-locking mechanism in the levelling actuator, which provides the driver with the option of low power consumption. Thus, when levelling is not activated, the actuator and the attached spring allow full wheel travel and do not consume power. Consequently, the damper actuator is fully active and is designed to act at higher frequencies, approximately >5 Hz.

4. Active suspension control law

A large amount of literature has been examined to regulate the quarter car model. Optimal control algorithms, such as LQ (linear quadratic regulator), have frequently been used to control the states of the sprung and unsprung masses under the influence of road disturbance [5,9]. A common strategy is to formulate cost functions to address the importance of different states and input signals. Since the dimensioning of the damper actuator is emphasised in this paper, the control gains will later be involved as well as the actuator parameters in the dimensioning process (further discussed in Section 6). Thus, the well established *Skyhook* control algorithm is adopted [9–11]. A wealth of research findings pose the query of whether this control strategy substantially contributes to comfort, while requiring few states to be measured. This is important, since full state feedback is hard to attain.

Before examining the *Skyhook* control task, the control problem can be closely scrutinised, where the controlled states can be assumed to be velocities and displacements of the sprung and unsprung masses [12]. In addition, road displacement is assumed to be involved as a state. Accordingly, this control law is thus formulated as

$$F_{\text{d}} = k_1 \dot{z}_{\text{b}} + k_2 z_{\text{b}} + k_3 \dot{z}_{\text{w}} + k_4 z_{\text{w}} + k_5 z_{\text{road}} \tag{3}$$

where $k_1 \ldots k_5$ are the state-feedback parameters of the controller. However, adopting this control law requires

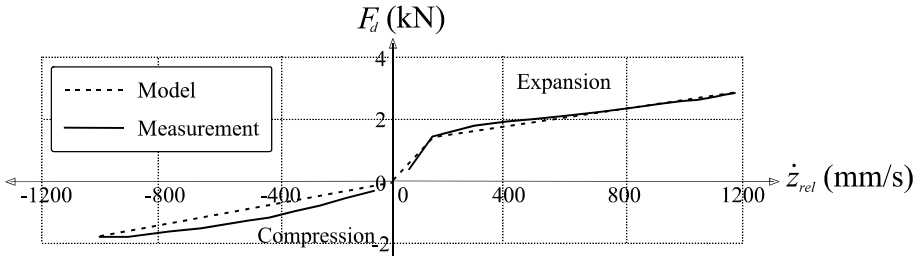

Fig. 4. A graph showing the damper force on the hydraulic damper studied.

measurements of all suspension states including road disturbance. Measurements of road disturbance, in particular, require sensor arrangements that are difficult to implement. Ideally, the car body should be isolated from road disturbances. However, for low frequency road irregularities, such as uphill slopes, the car body cannot be completely isolated due to the restricted wheel travel. This, for instance, is one of the reasons why it is difficult to involve the terms $k_2 z_b$ and $k_4 z_w$ in the active suspension control law. Added to which, absolute position sensors normally suffer from long-term drifting during the integral calculation from accelerometers used. Subsequently, this leads to an unacceptably low accuracy level.

The *Skyhook* control algorithm strives to anchor the car body relative to the sky, aiming to improve comfort. The anchor effect is produced by a force which resists the motion of the body. In contrast to a conventional damper, the *Skyhook* concept offers damping of the body without the transmission via the unsprung path. Nevertheless, since the *Skyhook* itself does not provide any damping of the wheel mass, it is advisable to include damping between wheel and body in the control law. Subsequently, the states required for the overall *Skyhook* damper are the relative wheel-to-body velocity and the absolute velocity of the body. However, according to the active suspension configuration illustrated in Fig. 3c, it is evident that the active damper (HB) coexists with the levelling actuator (LB) and the body spring, which both contribute to the total suspension force produced as follows:

$$F_{\text{susp}} = k_b(z_w - z_b) + k_l(z_w - z_b + z_l) + c(\dot{z}_w - \dot{z}_b) + c_{\text{sky}}\dot{z}_b \tag{4}$$

The first term in Eq. (4), corresponds to the passive spring between wheel and body. The second term is the force contribution from the levelling actuator, where an additional state, z_l, is introduced and defines the position of the levelling spring in relation to the levelling actuator. This spring has a stiffness of k_l (N/m). Finally, the two last terms with control gains c (N s/m) and c_{sky} (N m/s), are assigned to the active damper, which is supposed to be controlled by the *Skyhook* proposed. Hence, the control law given in Eq. (4) can now be re-expressed as

$$\begin{aligned} &F_{\text{susp}} = k_{\text{tot}} z_{\text{rel}} + F_l + F_d, k_{\text{tot}} = k_b + k_l \\ &F_l = k_l z_l \quad \text{and} \quad F_d = c(\dot{z}_w - \dot{z}_b) + c_{\text{sky}}\dot{z}_b \end{aligned} \tag{5}$$

where F_l is the generated force from the levelling actuator and F_d is the force from the damper actuator. Incidentally, for the purposes of this research, the authors have chosen not to consider the design and control of the levelling actuator.

5. Rotational dynamics of the active wheel suspension

The quarter car model described in Sections 3 and 4 only appraises linear actuator motions. Since the proposed implementation of the damper is a rotating electric machine, it is necessary to re-express the linear damper position in relation to the angle of the upper arm. In addition, the damper force is re-expressed to the corresponding damper torque.

The distance between the body position, z_b (position of the damper arm-body joint), and the position of the wheel, z_w (position of the arm-wheel joint), as defined in Section 3 (also see Fig. 5) is defined as

$$z_{\text{rel}} = z_w - z_b \tag{6}$$

This distance is indirectly measured using an encoder on the damper machine, which measures the angle of the damper arm, ϕ_a, (more specifically, ϕ_d, which is $\phi_a n_d$, as illustrated in Fig. 6). The distance, z_{rel}, and its derivatives are related to the damper arm angle as follows:

$$\begin{aligned} z_{\text{rel}} &= l_a \sin\varphi_a \\ \dot{z}_{\text{rel}} &= \dot{\varphi}_a l_a \cos\varphi_a \\ \ddot{z}_{\text{rel}} &= \ddot{\varphi}_a l_a \cos\varphi_a - l_a \dot{\varphi}_a^2 \sin\varphi_a \end{aligned} \tag{7}$$

A force acting in the vertical direction of the wheel, F_a, is translated into a torque, T_a, on the damper arm according to

$$T_a = F_a l_a \cos\varphi_a \tag{8}$$

5.1. Damper inertial forces and torques

In the quarter car model, the acceleration of the unsprung mass is directly related to its mass, m_w, which follows Newton's third law of motion. Due to the implementation of this, it is necessary to add the inertia of the damper e.g. machine, gears, shafts and arm, to the total unsprung weight. Hence a 'fictitious' mass, corresponding to the mass moment of inertia of the damper needs to be added to the unsprung mass of the quarter car model. The inertial torques, T_i, required to accelerate the damper inertia are given by

$$T_i = J_a \ddot{\varphi}_a \tag{9}$$

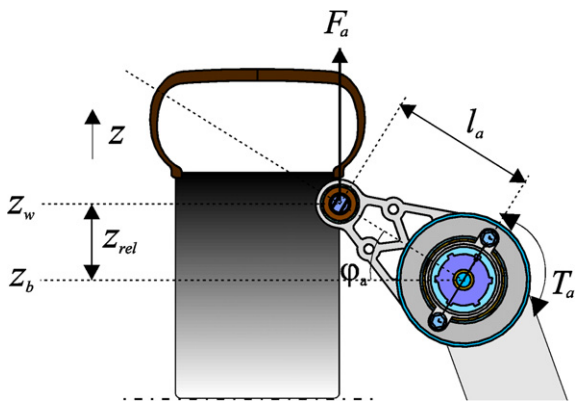

Fig. 5. Front view of wheel suspension geometry (simplified).

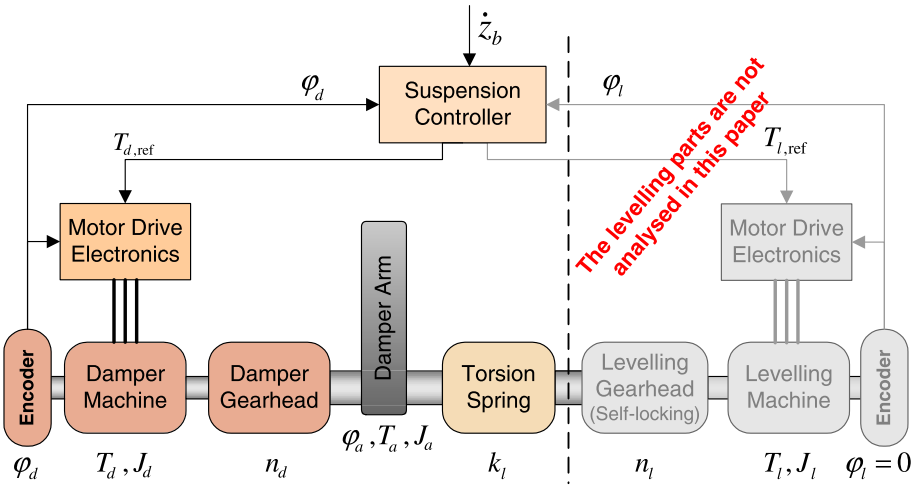

Fig. 6. Schematic of the active suspension system.

where J_a is the mass moment of inertia of the damper mechanism. Combining this expression with Eqs. (7) and (8), gives the corresponding force, F_i, on the wheel

$$F_i = \frac{J_a \ddot{\varphi}_a}{l_a \cos\varphi_a} = \frac{J_a}{l_a^2 \cos^2\varphi_a}\ddot{z}_w + \frac{J_a}{l_a^2 \cos^2\varphi_a}(l_a \dot{\varphi}_a^2 \sin\varphi_a - \ddot{z}_b) \quad (10)$$

In this equation, the first term can be regarded as a fictitious increase of the wheel mass, which must be added to the wheel mass in the quarter car model. It then follows that the last term of Eq. (10) contains the body acceleration, which is a problem, since the accelerations of the two masses (wheel and body) are assumed to be independent of each other (classic quarter car model, Eq. (1)). Fortunately, the amplitude of the accelerations of the body is much smaller than the amplitude of accelerations of the wheel, therefore the last term in Eq. (10) can be ignored, and the equation may be reformulated as

$$F_i \approx m_f \ddot{z}_w + m_f l_a \dot{\varphi}_a^2 \sin\varphi_a \quad (11)$$

where m_f represents the fictitious increase of the unsprung mass.

$$m_f = \frac{J_a}{l_a^2 \cos^2\varphi_a} \quad (12)$$

5.2. Damper torque

The contributions to the torque at the upper arm originate from; the damper machine, the inertial torque required to accelerate the damper arm and the torque generated in the torsion spring. The torsion spring is in parallel to the damper machine (Fig. 6). Hence, the torque at the upper arm is

$$T_a = T_d n_d + (\varphi_a - \varphi_l/n_l)k_l + T_i \quad (13)$$

where n_d and n_l are the damper and levelling gear ratios. The torque produced by the damper actuator is denoted as T_d. The torsion spring, which is attached to the levelling actuator, has a rotational stiffness, k_l, (N s/rad) and is tensioned by an angle, ϕ_l (rad). Since the levelling actuator is not analysed, ϕ_l is set to zero. The corresponding vertical force acting on the wheel and the body is formulated as

$$F_a = \frac{T_d n_d + \varphi_a k_l}{l_a \cos\varphi_a} + m_f l_a \dot{\varphi}_a^2 \sin\varphi_a + m_f \ddot{z}_w \quad (14)$$

The linear representation of the quarter car model (Sections 3 and 4) is now adapted to fit the rotational structure of the damper, which increases the unsprung mass to $m_w + m_f$. (see Section 5.1). Reformulating Eq. (1) for the active damper results in

$$\begin{aligned} m_b \ddot{z}_b &= F_{susp} - m_b g \\ (m_w + m_f)\ddot{z}_w &= -F_{susp} - m_w g + k_w(z_{road} - z_w) \\ z_{deflection,min} &< z_{road} - z_w < z_{deflection,max} \end{aligned} \quad (15)$$

where F_{susp} is given by

$$F_{susp} = F_a - m_f \ddot{z}_w + z_{rel} k_b \quad (16)$$

where k_b is the stiffness for the leaf spring illustrated in Fig. 2.

5.3. Damper power dissipation

The electrical dynamics of the machine are assumed to be much faster than the dynamics of the mechanical system. Thus, the electric machine is modelled as an ideal torque generator. However, it is necessary to model the losses in the machine in order to estimate the total energy consumption of the system. Losses in an electric machine may be classified into three categories: *copper*, *iron* and *friction* losses. For the sake of simplicity, only copper losses will be included in this analysis, since these losses usually comprise the largest source of heat generation in a

machine. For a three-phase machine the resistive losses are given by

$$P_{\mathrm{l,m}} = 3R_{\mathrm{p}}I_{\mathrm{p}}^2 \tag{17}$$

where R_{p} represents the winding phase resistance and I_{p} the phase current. The power electronics in the motor drive electronics is also a major heat source in an electromechanical servo system. Losses in the drive electronics may be classified into *switching* and *conduction* losses. Only conduction losses are considered since they are the most relevant to this study. Assuming MOSFET semiconductors and a three-phase machine, the conduction losses are approximated to

$$P_{\mathrm{l,pe}} = 3R_{\mathrm{on}}I_{\mathrm{p}}^2 \tag{18}$$

where R_{on} is the on-resistance in the transistors. The reduction gear is assumed to be much more rigid than the springs and its backlash is assumed to be small. Furthermore, the gear inertia is assumed to be small in comparison to the inertia of the electric machine. Hence, the gear is modelled as an ideal gear ratio, n. However, even in this case, it is necessary to have a model of the energy losses. Consequently, the power losses in the gear are assumed to be dominated by the Coulomb friction between the gear teeth in mesh, and it is modelled as

$$P_{\mathrm{l,g}} = \mu_{\mathrm{g}}|T_{\mathrm{a}}\dot{\varphi}_{\mathrm{a}}| \tag{19}$$

where μ_{g} represents the Coulomb friction coefficient. Finally, the total power developed from the heat in the damper is then given by

$$P_{\mathrm{loss}} = P_{\mathrm{l,m}} + P_{\mathrm{l,pe}} + P_{\mathrm{l,g}} \tag{20}$$

6. Dimensioning and optimisation

This section deals with the physical dimensioning of the damper actuator and the optimisation of the controller and spring parameters (Eq. (5)). It is a well-known and time-consuming dilemma to tune these wheel suspension parameters in vehicles. This provides a reason for the use of optimisation methods to assist designers in finding one optimal set of parameters with acceptable performance. The work presented in this section is mainly based on methods and models developed during previous research by one of the authors e.g. [13] and [14] thus will not be described in detail in this paper.

The design problem solved in this paper is a very complex one, since the controller parameters and the physical parameters of the actuator are to be optimised in the same process. Traditionally, a control problem is solved for an already existing physical system, where it is obvious that the parameters of a controller depend on the parameters of the physical system being controlled. However, if the design problem is extended to include the design and optimisation of the physical components (in this case the damper actuator), the opposite also becomes true. The parameters of the physical system depend on the parameters of the controller. For example, high controller gains lead to better performance but also to higher torque requirements, which makes a large actuator necessary. It is therefore impossible to separate the design of the physical components from the controller design and still reach an optimal system design. Consequently, in order to find a design solution close to the combined optimum of the controller and actuator, an optimisation process as shown in Fig. 7 is proposed.

The first step in Fig. 7, Optimisation Loop I, optimises the suspension model with respect to the objective function described below (Eq. (28)). The goal of this step of the optimisation process is to derive the design load of the damper actuator. In this initial stage the damper actuator is assumed to be ideal (zero inertia and no torque restrictions). The parameters to be optimised are the controller parameters and the spring rates of the leaf and torsion spring (c_{sky}, c, k_{l}, k_{b}). From this first optimisation, a load profile for the damper actuator is obtained, which is then used as input for the second step of the optimisation process, 'dimensioning'. The goal with this part of the optimisation process is to derive the optimal physical parameters of the damper actuator. Here, optimal refers to the design that minimises the total volume of the damper actuator.

Finally, the controller and the spring rates are once more optimised in the Optimisation Loop II, though they

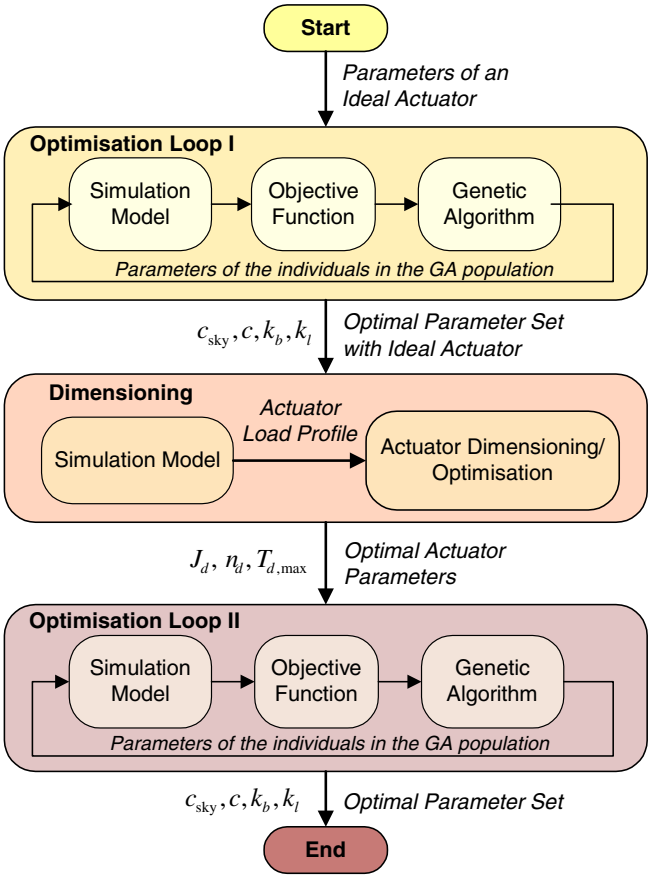

Fig. 7. Overview of the dimensioning and optimisation process.

now include the actuator parameters retrieved in the previous step. However, in order to retrieve the exact system optimum it is necessary to iterate between the optimisation of the physical components and optimisation of the controller according to the nested modelling approach described in [15]. During all stages of the dimensioning and optimisation process (Fig. 7), a road profile, z_{road}, (t) is required as input. The physical parts are dimensioned for continuous operations with respect to the road profile; hence the results of the dimensioning and optimisation process depend strongly on this profile. Using an extremely harsh road profile e.g. continuous driving on Belgian pavé, will result in an unrealistically large actuator. Hence the choice fell to a sinusoidal chirp signal according to Eq. (21) when dimensioning the physical parts.

$$z_{\text{road}} = (-0.18t + 2.5) \cdot 10^{-3} \sin(2\pi(0.9t + 2)) \tag{21}$$

Or plainly stated; a 10 s, sinusoidal frequency sweep from 2–11 Hz with amplitude of 2.5–0.7 cm, see also Fig. 8. Dimensioning and optimisation are carried out using a vehicle specification according to the parameter list in Appendix A.

6.1. Performance indices

In order to evaluate the performance of the suspension it is necessary to formulate some sort of evaluation criteria. The evaluation criteria must cover comfort and road holding capabilities as well as the energy consumption of the system. This entails the formulation of three different performance indices, χ. Two of them are based on the root-mean-square norm, which is defined as

$$|x|_{\text{rms}} = \sqrt{\frac{1}{\tau}\int x^2 \,\mathrm{d}t} \tag{22}$$

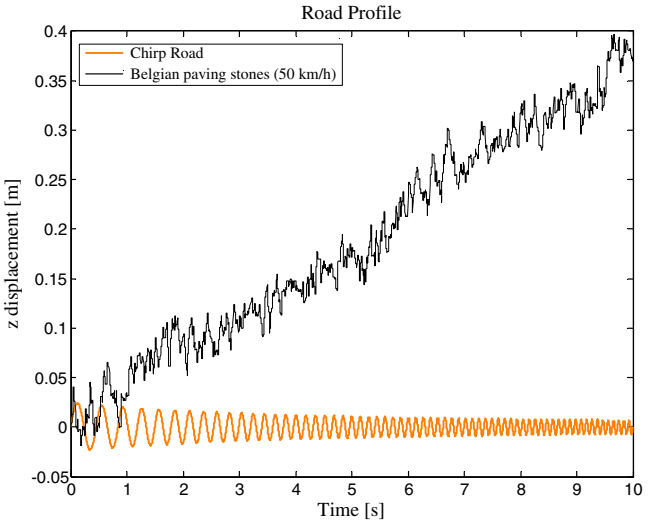

Fig. 8. Chirp road profile according to Eq. (21) and profile of a paved road similar to Belgian pavé at 50 km/h (the low-frequency inclination of the graph is a result from tests on slopes).

Comfort is strongly related to the accelerations of the vehicle body, therefore the performance index for comfort, χ_{ba}, is formulated as

$$\chi_{\text{ba}} = \frac{|\ddot{z}_{\text{b,active}}|_{\text{rms}}}{|\ddot{z}_{b,\text{passive}}|_{\text{rms}}} \tag{23}$$

As seen in Eq. (23), the comfort index is weighted with respect to the acceleration of the body in a conventional system, which is described in Eq. (2). A value above 1 means that the performance of the active suspension is considered to be inferior compared with the passive suspension.

Road holding capability is directly related to the variation in vertical tyre force. A constant tyre force, F_{t}, is ideal. In addition, the index, χ_{tf}, is weighted with respect to the passive suspension and is given below

$$\chi_{\text{tf}} = \frac{|F_{\text{t,active}}|_{\text{rms}}}{|F_{t,\text{passive}}|_{\text{rms}}} \tag{24}$$

where F_{t} is given by

$$F_{\text{t}} = k_{\text{w}}(z_{\text{w}} - z_{\text{road}}) \tag{25}$$

To attain a low energy consumption, it is important that the energy dissipated in the system is as low as possible. Hence, the third index, χ_{en}, is based on the power loss in the system, expressed as the ratio between the losses in the active and the passive designs, see Eq. (20)

$$\chi_{\text{en}} = \frac{\int P_{\text{loss,active}}}{\int P_{\text{passive}}} \tag{26}$$

These three indices are combined to form an objective function for the optimisation algorithm used later on. In order to avoid poorly performing solutions, indices over 1 are penalised according to Eq. (27). In the objective function, f (Eq. (28)), each performance index is combined with a weight, $\boldsymbol{w} = [w_1\, w_2\, w_3]$ (comfort, road holding and energy). These weights are used to rank the different indices in order of importance. For example, by choosing $\boldsymbol{w} = [2\,1\,1]$, a greater importance is given to maintain body acceleration at a lower level than the variation in tyre force and energy consumption.

$$\left.\begin{aligned} \chi_{\text{i}} &\geqslant 1 \\ \chi_{\text{i}} &< 1 \end{aligned}\right\} \begin{aligned} \chi_{\text{i}} &= \chi_{\text{i}}^3 \\ \chi_{\text{i}} &= \chi_{\text{i}} \end{aligned} \tag{27}$$

$$f = w_1\chi_{\text{ba}} + w_2\chi_{\text{tf}} + w_3\chi_{\text{en}} \tag{28}$$

6.2. Controller optimisation

The optimisation technique used for the optimisation of the controller parameters and the spring rates is based on a genetic algorithm (GA). The main advantage of this method and all other non-gradient based optimisation methods is that it does not need the derivatives of the objective function, which are difficult to calculate from a numeric simulation model. The basic idea of genetic algorithms is the mechanism of natural selection e.g. [16] and

[17]. Each optimisation parameter is coded into a gene, in this case, a real number. The corresponding genes for all parameters form a chromosome which describes each individual, accordingly:

$$\text{Chromosome} = [\, c_{\text{sky}} \quad c \quad k_{\text{b}} \quad k_{\text{l}} \,].$$

Each individual represents a possible solution, and a set of individuals are called a population. For each individual in the population, the value of the objective function is calculated. The best individuals are selected for mating, which is performed by combining genes from different parents to produce a child. Random mutations may also occur. Finally the offspring is inserted into the population and the process starts all over again until the maximum number of generations has been reached.

During the process of this research, the authors used the genetic algorithm implemented in the MATLAB [1] GEAtbx toolbox [18]. The genetic optimisation loop, as seen in Fig. 6, is executed twice. First, the simulation model is executed using parameters of an ideal actuator ($J_{\text{m}} = 0$, $T_{\max} = \infty$). The intention of this is to obtain an estimated load profile of the damper, which is necessary for dimensioning the electric machine and gear. In the former, weight vector for the objective function, formulated in Eq. (28), is set to, $\boldsymbol{w} = [10\,1\,0]$. In other words, the focus is on comfort, yet the non-linear characteristics of the indices presented in Eq. (27) maintain its road holding capability reasonably well.

6.3. Design and optimisation of the physical components

The dimensioning and optimisation method used to retrieve the minimum sizes of the damper machine and gearhead is presented in detail in [13]. The method for machine optimisation is based on a scaling approach where data from a real electric machine is scaled to fit the application exactly. The machine dimensions required are calculated as a function of the gear ratio to be able to select the best motor and gear ratio combination. The size of each gear is calculated using gear sizing models based on the Swedish standard for spur gear dimensioning, which is also presented in [13].

It is necessary to obtain input for the sizing method; a load profile representing the required torque and speed of the actuator as a function of time. In this case, such a profile is obtained by simulating the system using the controller parameters obtained in the previous section. Furthermore, a machine type has to be selected. In this case, the choice fell to a permanent magnet synchronous AC machine, mainly as it is known to have a high torque density, low inertia and good controllability. A three-wheel planetary gear train is selected for the damper gear since it is known to be compact and is highly efficient.

[1] MATLAB is registered trademark of The Mathworks Inc., Natick, Massachusetts, USA.

The optimisation process adopted for the machine and gear selected has resulted in a relation between weights and gear ratio, which is illustrated in Fig. 9. From this figure it is evident that the total weight of the machine and the gearhead decreases as gear ratios increase. However, the maximum gear ratio is limited by the restrictions of the maximum rotational speed of the electric machine. The smallest (lightest) machine/gear combination that lies within the operational speed range is selected for further evaluation (gear ratio = 19).

In Table 1, machine and gear data is shown in the row highlighted. Results indicate that the damper becomes relatively large and heavy. The size of the electric machine is governed by the amount of energy dissipated, while the gearhead size depends on peak loads only. However, one way to reduce the size of the actuator is to consider involving a conventional hydraulic damper combined with the electric damper proposed (Fig. 10). Since the hydraulic damper will partly contribute to the damper rate, c, the load profile of the electric damper will be relieved. The second row in the table shows the results from the dimensioning of the electric damper with a parallel hydraulic damper with $c = 763$ N s/m. It is evident that the size of the electric damper has been significantly lowered. However, the drawback of this solution is that the damping parameters cannot be as freely changed during driving as in a pure electric solution.

Since the size of the gearhead mainly depends on peak loads, those can be limited by the introduction of slipping friction bearings. These bearings protect the gearhead from destruction especially in severe driving conditions.

Thus far, the actuator has been dimensioned for continuous operation using the Chirp road profile described in Eq. (21) and Fig. 8. This means that the machine will overheat during continuous driving on rougher road

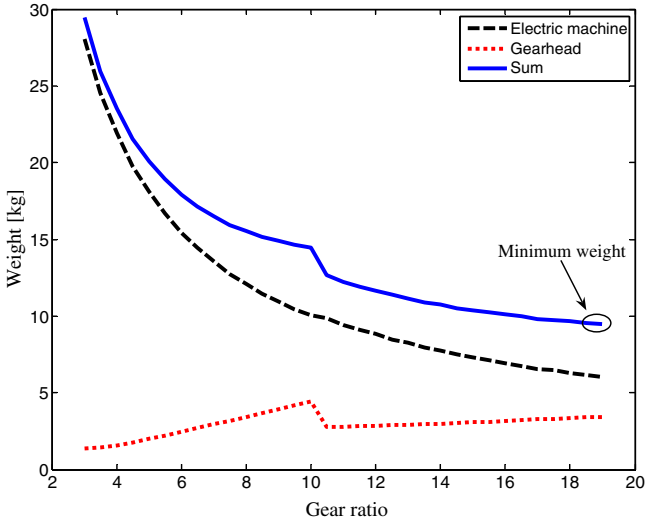

Fig. 9. Component weights as a function of gear ratio (the discontinuities at gear rate = 10 are caused by the need of an extra set of gears connected in series).

Table 1
Sizes of the damper machine and gearhead for three different design cases

Design case	$T_{d\ [rms]}$ [N m]	n_d	T_{rated} [N m]	m_m [kg]	l_m [mm]	r_m [mm]	m_g [kg]
Electric damper	87.1	19	4.6	6.0	157	40	1.6
Electric + hydraulic dampers	29.1	29	0.85	1.4	98	25	1.6
Electric damper, pavé conditions	158	19	10.4	12	197	49	3

Weights and dimensions represent active parts only, weights of bearings, housing, shafts, etc. have been intentionally ignored (the nomenclature list is shown in Appendix A).

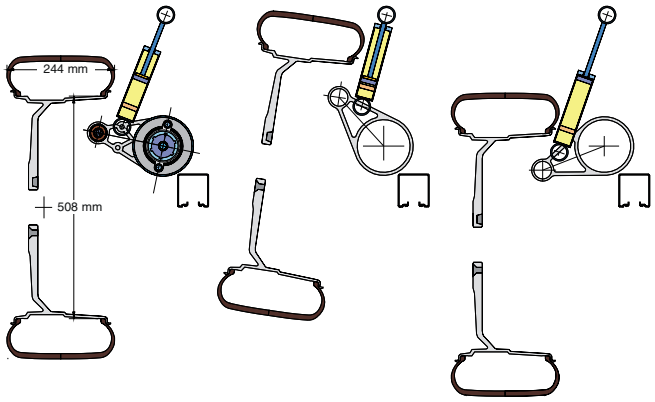

Fig. 10. Combined electric and hydraulic damper (illustrations reproduced with kind permission from Sigvard Zetterström at KTH, Sweden).

conditions. For purposes of comparison, an actuator has been dimensioned for continuous driving on a paved road (Belgian pavé, Fig. 8), which is known to be a very thorough damper test and often used for reliability studies. The third row in Table 1 shows the resulting actuator parameters. This actuator will in all likelihood handle any type of driving without overheating. However, since these extreme driving conditions are very rare, a better way to avoid overheating might be to reduce the controller gains when the electric machine has been under large loads for a long time. This strategy will decrease performance but save the actuator from damage. For the following sections in this paper, the actuator specifications in Table 2 and the first row in Table 1 will be used.

Up to this stage, effects of the voltage supply have not been commented. Though it is clear that the supply voltage mostly affects the cross-sectional area of the feed wires to the system. A low voltage causes high currents and therefore heavy cables and cumbersome wiring. It may also be hard to design large machines for low voltages. In this case, no voltage level is assumed, but the electric data on the machine has been retrieved from a machine designed for a 300 V DC supply.

Table 2
Data on the selected electric machine design (in addition to row 1, Table 1)

Machine parameter	T_{rated} [N m]	T_{peak} [N m]	R_p [Ohm]	k_t [N m/A]	J_d [kgcm^2]
	4.6	23	1.1	0.61	4.3

Table 3
Results of the controller optimisation with respect to three different weight vectors

Focus	$\boldsymbol{w}$	c [N s/m]	c_{sky} [N s/m]	k_b [k N/m]	k_l [N m/rad]
Comfort	[10 1 1]	640	9007	19.3	324
Handling	[1 10 1]	1623	1578	22.3	600
Energy	[2 1 3]	822	482	24.8	212

The last step in the dimensioning and optimisation process is to optimise the controller and suspension parameters once again, since the dynamics of the system will have changed with the extra inertia of the electric damper machine. To illustrate the process, the authors will define three different weight vectors and are listed as follows: *comfort*, *handling* and *energy*, see the column $\boldsymbol{w}$ in Table 3. Results from the controller optimisation using the three different weight vectors, are also shown in Table 3.

7. Evaluation

The evaluation of the proposed active suspension is carried out according to a vehicle specification found on the parameter list in Appendix A. For purposes of comparison and as a reference, the passive suspension has also been evaluated. However the passive suspension parameters have not been optimised, since it is assumed that this configuration is matched and tuned to perfection through the development of it.

7.1. Transmissibility of road disturbances

To evaluate the ability of the active electric suspension to suppress road disturbances, the vehicle has been subjected to sinusoidal road profiles of various frequencies. Fig. 11 shows the non-linear frequency responses of car body displacement and acceleration respectively, during the influence of road disturbances, z_{road}, with amplitudes of 1 cm (which ensure that the damper actuator is not saturated). The frequency response has been performed in the time-domain by calculating the steady-state amplification of these disturbances. The electric damper has been evaluated for the different weight vectors used in Table 3. As illustrated in Fig. 10, the active damper suppresses road disturbance to the car body satisfactorily. The damper with the *comfort* specifications performs better than the passive damper over the frequency range presented, which confirms the expectations of the authors. For the *handling* and *energy* specifications, the suppression of road disturbances is better for parts of the frequency band only. It is interesting to note that all specifications for the electric damper evaluated are seldom able to reject disturbances around the wheel hop resonance frequency (approximately 10 Hz). This property is coupled to the control law used (*Skyhook*), which by its definition is scarcely able to tackle

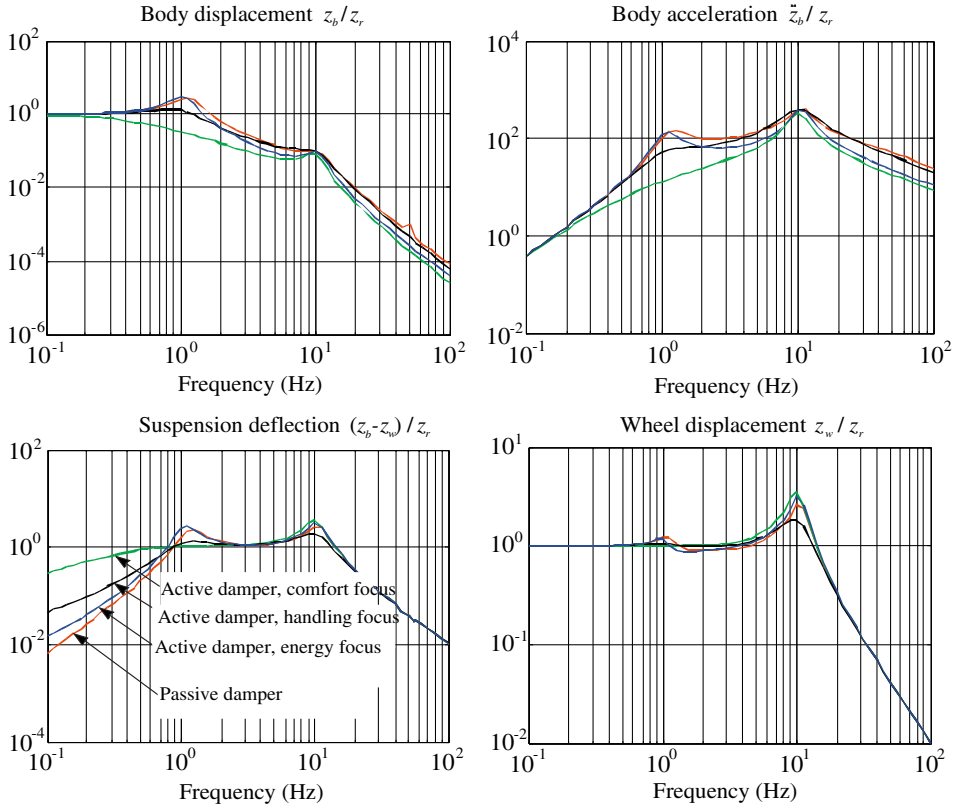

Fig. 11. Transmissibility of road disturbance for the passive system as well as results from the solutions found from the optimisation process when either the *handling*, *comfort* or *energy* criteria were used (see Table 3).

the wheel resonance. Moreover, the *comfort* specified active damper has a larger wheel displacement than the passive damper. Hence, the tyre force variation will be larger even if the ride is satisfactory. On the other hand, if c_{sky} is reduced and c increased when handling the weight vector, the wheel displacement can be lowered at the expense of a comfortable ride, which clearly demonstrates the conflicting demands of comfort and handling.

In addition, the electric damper is evaluated by its response to a step road profile. This condition is relevant for driving scenarios with e.g. bumps present. As seen from Fig. 12, the step of 2.5 cm is tackled very differently, where the *comfort* specified electric damper follows the road without overshooting at all. This response depends on the relatively high Skyhook damping. However, this occurs at the expense of large variations in tyre force, which is seen in Fig. 13. In this situation, the electric dampers with the weight vectors *energy* and *comfort* both level out the tyre force variation at a reduced rate than is realised by the passive suspension. Moreover, it is notable that the *energy* specified electric damper also follows the road with significant overshoots, which indicates that both low energy consumption and satisfactory performance cannot be maintained for this specific road disturbance.

7.2. Damper energy consumption

The energy consumption of the damper is given by the mechanical energy developed added to the losses in the system

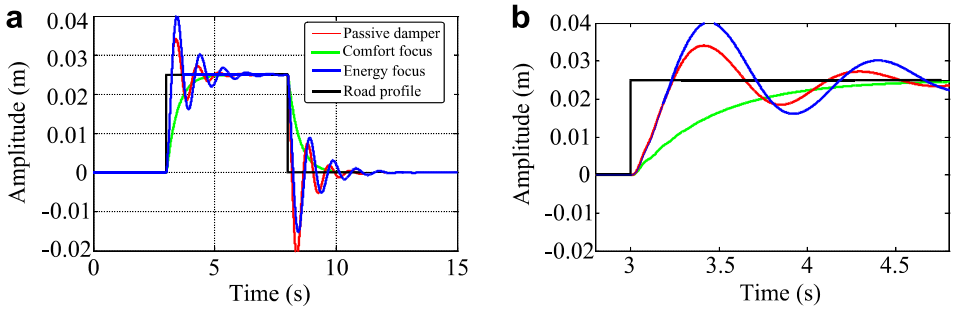

Fig. 12. Car body displacement when entering a stepped road profile for the studied damper criteria (enlarged illustration in (b)).

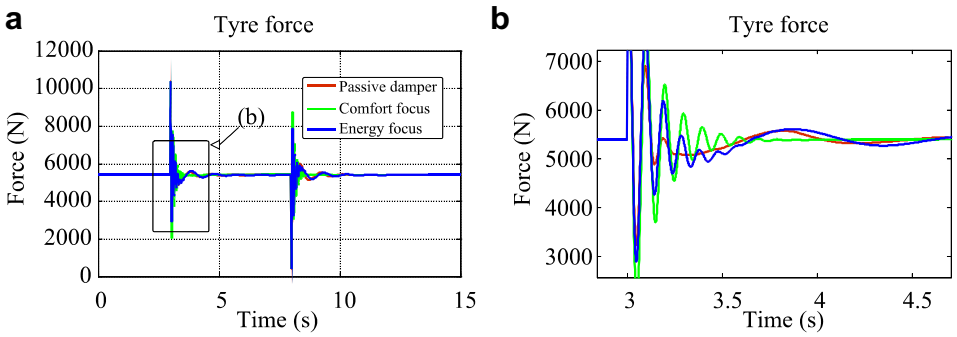

Fig. 13. The tyre force response to a stepped road profile for the damper criteria studied (enlarged illustration in (b)).

Table 4
Energy consumption during 10 s on Belgian Pavé (Fig. 8) and for a sinusoidal road profile

Energy [kJ]	Belgian Pavé				Sinusoidal (4 Hz 1 cm)			
	Comfort	Handling	Energy	Passive	Comfort	Handling	Energy	Passive
Mechanical (E_{mech})	−7.4	−7.1	−6.7	−7.0	−0.33	−0.68	−0.33	−0.66
Heat (E_{loss})	3.6	5.7	2.7	7.0	0.20	0.58	0.14	0.66
Electrical (E)	−3.8	−1.4	−3.9	N/A	−0.13	−0.10	−0.19	N/A

The table provides the consumption for the three control settings presented in Table 3 and for the passive suspension.

$$E = E_{mech} + E_{loss} = \int_0^{\tau} T_d \dot{\varphi}_d \, dt + \int_0^{\tau} P_{loss} \, dt \tag{29}$$

where P_{loss} is assumed to be dissipated as heat and is given by Eq. (20). Table 4 summarises the energy consumption for the three different controller settings presented in Table 3. In addition, the conventional hydraulic passive damper is added as a comparison. This process proves that energy consumption is always negative which indicates that the damper regenerates electricity. It is shown that heat dissipation is larger for the *handling* setting that for the *comfort* setting, see Table 4. The road conditions in Table 4, in particular for Belgian pavé, are considered to be more irregular than normal, which may explain the relatively high electrical energy regenerated.

8. Conclusions and future work

This paper has given an account of and discussed the opportunities available with the implementation of an electromechanical wheel suspension. A suitable dimensioning method of the control and actuator parameters by using genetic optimisation has also been included. In addition, this dimensioning method benefits from calculating the parameters of passive components, such as, different stiffnesses for wheel suspensions. It has been demonstrated that the preferred compromise between comfort, handling and energy dissipation can be controlled by the adaptation of the dimensioning method concerning the control and actuator parameters during the development process. The electric damper has been evaluated by studying the transmissibility of road disturbances to the car body. The evaluation showed a significant improvement of the car body isolation. However, due to the control law adopted, the transmissibility of road disturbances close to the wheel-hop frequencies does not provide greater benefit to the vehicle than passive suspension usage.

Since the energy dissipation models are involved in the design process of the electric damper, high energy dissipation design solutions can be avoided. It is interesting to note that the heat generated in the electric damper is lower than in the conventional passive suspension. Even though both configurations dissipate similar amounts of mechanical energy, the electric damper is able to regenerate parts of the mechanical energy to electricity. The results indicate a large electrical machine design, which is considerably difficult to package in a vehicle. However, if the electric damper is combined with a hydraulic damper and this combination is allowed to function during peak loads, then the size of the electric damper may be considered acceptable.

Bearing in mind the findings above, further research should focus on the feasibility to introduce smaller electrical machines without reducing damper performance. It is worth considering whether the wheel suspension geometry can be modified to lessen actuator peak loads and in turn reduce the actuator size. In addition, if short-term degradations of comfort are acceptable and if control parameters are allowed to be adjusted on-board, there is great potential to be able to reduce the size of the actuator damper even further.

Acknowledgements

This work was financed in part by the Swedish National Energy Agency and the Swedish National Green Car Pro-

gramme. The authors are grateful to Mr Sigvard Zetterström at KTH (former VCC) for his immense support and valuable comments. In addition we would like to thank Professor Annika Stensson Trigell and Professor Jan Wikander at KTH for their constant support.

Appendix A

Nomenclature

C damper rate [N s/m]
c_{sky} *Skyhook* damper rate [N s/m]
E, E_{mech}, E_{loss} Energy, mechanical work and energy losses [J]
F_a vertical force at the wheel/upper arm joint [N]
F_d, F_l damper and levelling actuator force [N]
F_t vertical tyre force [N]
F_{susp} suspension force [N]
f objective function
I_p phase current [A]
J_a damper arm inertia [kg m^2]
J_d, J_l damper and levelling actuator inertia [kg m^2]
$k_1 \ldots k_5$ control parameters for active suspensions [N s/m, N/m]
k_{tot} combined spring rate for body and levelling spring [N/m]
l_m damper electrical machine length [m]
m_f upper arm fictitious mass [kg]
m_m, m_g damper electrical machine and gear head mass [kg]
n_d, n_l gear head ratios for damper and levelling actuator
P power [W]
$P_{l,m}$, $P_{l,pe}$, $P_{l,g}$ resistive, conduction and Coulomb friction power losses [W]
P_{loss} total heat dissipation [W]
R_{on} transistor on-resistance [Ohm]
R_p winding resistance [Ohm]
r_m damper electrical machine diameter [m]
T torque [N m]
t time [s]
T_a upper arm torque [N m]
T_i upper arm inertia torque [N m]
T_d, T_l damper and levelling actuator torque [N m]
$w_1 \ldots w_3$ weights for the performance indices
z_b car body position [m]
z_l linear levelling actuator position [m]
z_w wheel position [m]
z_{rel} wheel position relative to the car body [m]
z_{road} road position [m]
ϕ_a the upper arm angle of the suspension [rad]
ϕ_d, ϕ_l damper and levelling rotor angle [rad]
τ cycle time [s]
χ_{ba}, χ_{tf}, χ_{en} performance index for body acceleration, tyre force variations and energy consumption
μ_g Coulomb friction coefficient

Parameters

G gravitational constant 9.81 [m/s^2]
k'_b body spring rate for the passive suspension 23 [k N/m]
k_w tyre spring rate 200 [k N/m]
m_b, m_w a quarter of the car body sprung and unsprung masses 500, 50 [kg]
$z_{deflection,max}$, $z_{deflection,min}$ Max and min tyre deflection 0.08, 0 [m]
$z_{rel,max}$, $z_{rel,min}$ Max and min relative displacement of wheel to car body −0.1, 0.1 [m]

References

[1] Williams RA. Automotive active suspensions Part 1: basic principles. Proc Inst Mech Eng, Part D 1997;211(6):415–26.
[2] Hsu P. Power recovery property of electrical active suspension systems. Energy conversion engineering conference, IECEC96. In: Proceedings of the 31st Intersociety, vol. 3, 1996. p. 1899–904.
[3] Baumal AE, McPhee JJ, Calamai PH. Application of genetic algorithms to the design optimization of an active vehicle suspension system. Comput Meth Appl Mech Eng 1998;163(1):87–94.
[4] Fathy HK, Papalambros PY, Ulsoy AG, Hrovat D. Nested plant/controller optimization with application to combined passive/active automotive suspensions. In: Proceedings of the IEEE American control conference, vol. 4, June, 2003. p. 3375–80.
[5] Poussot-Vassal C, Sename O, Dugard L, Ramirez- Mendoza R, Flores L. Optimal skyhook control for semi-active suspensions. In: Proceedings of the 4th IFAC symposium on mechatronics, Heidelberg, Germany, September, 2006.
[6] Zetterström S. Vehicle wheel suspension arrangement, Patent Number: EP1144212, 1998.
[7] Zetterström S. Electromechanical steering, suspension, drive and brake modules. In: Proceedings of the 56th IEEE vehicular technology conference, vol. 3, Vancouver, Canada, 2002. p. 1856–63.
[8] Zetterström S, Jonasson M. Method and arrangement for controlling a suspension of a vehicle wheel. Patent pending, Application no. 06126948-6, 2006.
[9] Crosby M, Karnopp D. The active damper – a new concept in shock and vibration control. Shock Vibr Bull 1973;43:119–33.
[10] Hudha K, Jamaluddin H, Samin PM, Rahman RA. Effects of control techniques and damper constraint on the performance of a semi-active magnetorheological damper. Int J Vehicle Autonomous Syst 2005;3(2–4):230–52.
[11] Tillback LR, Brodd S. Active suspension – the volvo experience. SAE Technical paper 890083, 1989.
[12] Lizell M. Dynamic leveling for ground vehicles, a low power active suspension system with adaptive control. Dissertation thesis, TRITA-MAE-1990-9, ISSN 0282-0048, Department of machine elements, KTH, Sweden, 1990.
[13] Roos F, Towards a methodology for integrated design of mechatronic servo systems, Doctoral thesis, TRITA-MMK 2007:07, ISRN/KTH/MMK/R-07/07-SE, KTH, Stockholm, Sweden, 2007.
[14] Roos F, Wikander J. The influence of gear ratio on performance of electromechanical servo systems. In: Proceedings of the 4th IFAC symposium on mechatronic systems, Heidelberg, September 2006.
[15] Fathy HK, Reyer JA, Papalambros PY, Ulsoy AG. On the coupling between the plant and controller optimization problems. In: Proceedings of the american control conference, vol. 3, 2001. p. 1864–69.
[16] Cominos P, Munro N. PID controllers: recent tuning methods and design to specification, IEEE. Proc Control Theo Appl 2002;149(1).
[17] Da Silva W, Acarnley P, Finch J. Application of genetic algorithms to the online tuning of electric drive speed controllers. IEEE Trans Ind Electron 2000;47(1).
[18] GEATbx (The genetic and evolutionary algorithm toolbox for Matlab), <www.geatbx.com>, 2007 (accessed 10.01.07).